High-pressure CO_2 excess sorption measurements on powdered and core samples of high-rank coals from different depths and locations of the South Wales Coalfield

Renato Zagorščak, Hywel R. Thomas*

Geoenvironmental Research Centre (GRC), School of Engineering, Cardiff University, The Queen's Buildings, The Parade, Cardiff, CF24 3AA, United Kingdom

KEYWORDS: Coal, Carbon sequestration, Anthracite, High pressure, Sorption, CO_2

ABSTRACT:

The experimental analysis aimed at investigating the high-pressure (sub- and super-critical) CO_2 sorption behaviour on two high-rank coals of different sizes is presented in this paper. Coals from the same seam (9ft seam), but from depths of 150 m (BD coal) and 550 m (AB coal) and different locations of the South Wales (UK) coalfield, known to be strongly affected by tectonically developed fracture systems, are employed for that purpose. Hence, the sorption behaviour of powdered (0.25-0.85 mm, 2.36-4.0 mm) and core samples obtained from locations associated with the deformation related changes is analysed in this paper to assess the CO_2 storage potential of

such coals. The results show that the coals exhibit maximum adsorption capacities up to 1.93 mol/kg (BD coal) and 1.82 mol/kg (AB coal). No dependence of the CO_2 maximum sorption capacity with respect to the sample size for the BD coal is observed, while for the AB coal the maximum sorption capacity is reduced by more than half between the powdered and core samples. The CO_2 sorption rates on BD coal decrease by a factor of more than 9 from 0.25-0.85 mm to 2.36-4.0 mm and then remain relatively constant with further increase in sample size. The opposite is observed for the AB coal where sorption rates decrease with increasing sample size, i.e. reducing by a factor of more than 100 between the 0.25-0.85 mm and core samples. The differences in behaviour are interpreted through the structure each coal exhibits associated with the burial depths and sampling locations as well as through the minor variations in ash contents. This study demonstrates that anthracite coals, having experienced sufficient deformation resulting in changes in fracture frequency, can adsorb significant amounts of CO_2 offering great prospect to be considered as a CO_2 sequestration option.

1. Introduction

In view of the recent reports on the impacts of global warming, it is expected that at around 810 Gt of CO_2 will have to be stored until 2100 to limit the rise in temperature to 1.5°C on pre-industrial times[1, 2]. Consistent with the UK's leadership role in the global climate change agenda, the UK would need to reach net-zero emissions of CO_2 by about 2050[2]. Hence, to meet those ambitions and minimise the negative impacts of climate change on people and the environment, active removal of greenhouse gases from the atmosphere and their storage is required.

Carbon Capture and Storage (CCS) technology is a cost-effective solution able to deliver emissions reductions from the use of fossil fuels[3]. Coals are considered as dual porosity systems consisting of a porous matrix and a network of natural fractures and as such offer a great prospect of storing gases. Although small amounts of free gas may exist in the coal fracture system, gas is mainly adsorbed on the internal surface area of the coal matrix accounting for 95-98% of the gas in the coal seam[4]. The porosity distribution is coal rank-dependent with low rank coals mainly containing macropores, while high rank coals contain predominantly micropores which offer most of the surface area where gas can adsorb[4]. Porosity can be also associated with maceral groups whereas vitrinites are mainly composed of micropores, while liptinites and intertinites are predominantly formed of mesopores and macropores[4, 5]. Consequently, the bright, vitrinite-rich coals have higher sorption capacity both for methane and carbon dioxide than dull, inertinite-rich coals[5]. Coal seams are also characterized by fractures which usually occur in two sets mutually perpendicular, i.e. face cleats which are the dominant fracture system and butt cleats[6, 7]. Cleat development is related to the coal rank as the cleat frequency increases from lignite to low volatile bituminous coal and then decreases as the rank increases further to anthracite which has a direct impact on permeability which increases with increasing cleat frequency[6, 7]. Therefore, it is generally assumed that anthracite, despite high amounts of micropores and consequently high sorption capacity to gases, is unsuitable for gas production or storage due to low fracture permeability and wide cleat spacing which increases the mean diffusion distance between the pores and fractures[8].

Although regions hundreds of square kilometers in area can have uniform cleat orientations, the cleat network can shift abruptly from one coal seam to the next within an area as small as a single colliery[6]. In addition, localized shear zones or tectonically developed fracture systems can

dramatically change the permeability[7]. Furthermore, fracture intensity and size can locally vary depending on the position on folds and proximity to faults[6]. If large continuous areas of such high rank coals are present, they may offer significant methane sources and carbon dioxide sinks owning to the increase in inherent permeability due to tectonically induced fracture sets. This study therefore investigates the CO_2 sorption behaviour of high-rank coals, obtained from the same coal seam, but from different depths and locations of the South Wales coalfield known to be affected by deformation to provide further understanding of the storage potential of such coals.

Determining the sorption amount of CO_2 that can be stored in a particular coal seam and the kinetics of sorption are important steps in assessing the potential of the coal seam for the sequestration purpose. Such sorption capacity estimation must be performed under relevant conditions as the depth interval for CO_2 storage is between 700 m and 1500 m of depth, where pressure and temperature would exceed the critical values of carbon dioxide, i.e. 7.39 MPa and 31.1°C, respectively[4]. Most of the experimental investigations were focused on gas sorption capacity of powdered coal samples where the sorption process is expected to be relatively faster compared to larger samples[9-18]. However, the sorption capacity values obtained on powdered samples may not represent the values obtained on intact coal samples, as shown through the works of researches who have conducted experiments on coal samples of different sizes including core samples[17, 19-25]. While some researchers did not observe any general trend of the sorption times and sorption isotherms with respect to particle size[24], others suggested that increasing the sample size lowers the sorption capacity and kinetics as less micro-pores are either available or accessible[17]. Hence, this paper aims to provide further insights into the sorption behavior of both intact and powdered high-rank coal samples of different sizes.

The results of a series of carbon dioxide sorption measurements up to 8.7 MPa using the manometric sorption apparatus are presented. The behaviour of powdered coal samples with grain sizes of 0.25-0.85 mm and 2.36-4.0 mm, and coal cores obtained from two different coal mines are analysed. The pressure decay curves are obtained and the time for the gas pressure to reach equilibrium is discussed and compared for samples of different sizes, locations and depths. Based on the values of gas pressures injected into the system during each injection step and pressure decay experimental results, the excess and absolute sorption values as a function of equilibrium pressure on all samples are presented and analysed. The absolute sorption capacities are quantified by applying fitting curves to the experimentally determined values and obtaining the parameters related to the increase in sorption capacity as a function of gas pressure. The kinetic aspects of CO_2 sorption on samples of different sizes are explored using first-order and second-order rate functions. Using these functions, fitting parameters related to the kinetics of CO_2 sorption are obtained and analysed.

2. Experimental Methodology

2.1.Samples

Coal blocks were collected from two different coal mines in the South Wales coalfield which extract coal from the 9ft seam[26, 27]. Coal extracted from the 150 m depth is from the East Pit Mine, located in the NW outcrop of the South Wales coalfield, and is locally called the Black Diamond (BD), while coal extracted from the 550 m depth is from the Aberpergwm mine (AB), located 16 km away in the SE direction (Figure 1).

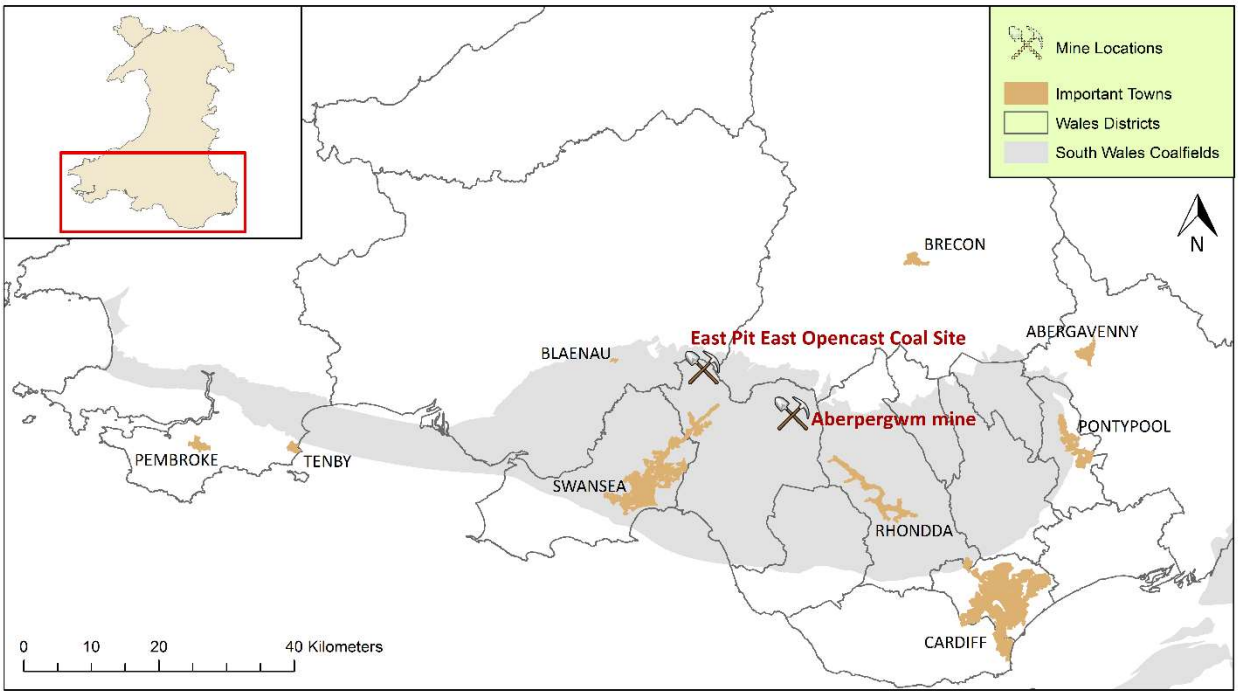

Figure 1. South Wales coalfield and the coal sampling locations[27].

From the coal blocks obtained, both powdered and core samples were prepared for this research. The preparation and air-drying of coal samples was conducted following the ASTM[28] standard of practice. For the purpose of the sorption experiments, coal samples were crushed and divided into two different grain sizes, i.e. 0.25-85 mm and 2.36-4.0 mm (Figure 2a). Powdered coal mass of 50 g was used for each experiment.

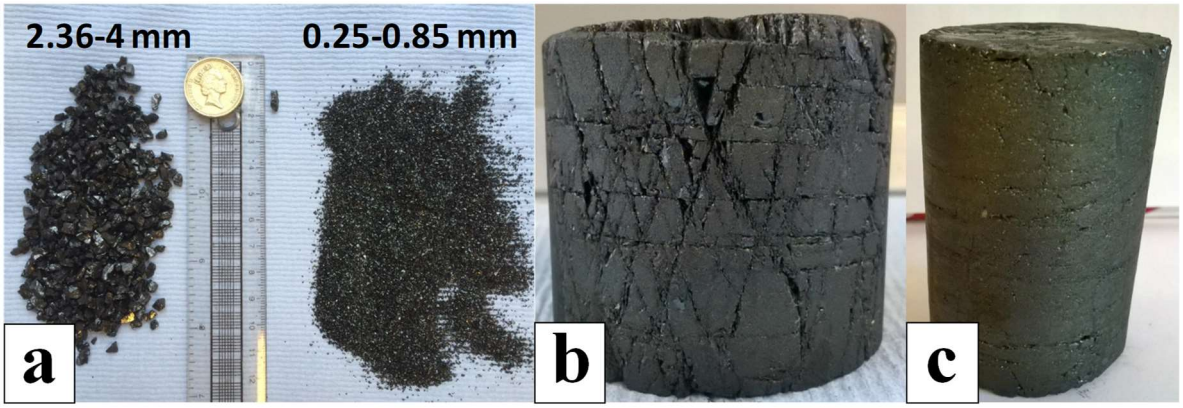

Figure 2. Coal samples used for the sorption experiments; a) Powdered samples, b) BD core, c) AB core.

Coal cores were drilled out of the coal blocks using a coring machine and applying a tap water as a cooling agent while drilling. Two diamond core drilling bits with different internal diameters, i.e. 44 mm and 36 mm were used to obtain the coal cores from the BD (Figure 2b) and AB (Figure 2c) blocks, respectively. Upon extraction, cores were cut to their required lengths, 38 mm for the BD sample and 53 mm for the AB sample, using a diamond circular saw. The difference in diameters and lengths is related to the fact that during the drilling of the BD coal block, it was very challenging to produce the 36 mm sample due to the fractured nature of the BD coal. Hence, it was decided to use the next larger drilling bit available in the laboratory to obtain the sample that could be used in the sorption cell. However, despite the difference in diameters and lengths, the primary aim was to obtain samples of similar volumes and masses, i.e. AB core is 79.3 g and BD core 74.2 g. Based on the measured dimensions and weights, the resulting density values of the respective samples were approximately 1362 $kg.m^{-3}$ for the BD sample and 1368 $kg.m^{-3}$ for the AB sample.

Proximate, ultimate, petrographic and calorimetric analyses were conducted to characterise the coals (Table 1). Both coals exhibit very similar properties with the main difference being the ash content, i.e. 1.65% for the BD coal and 4.62% for the AB coal. Based on the results obtained and

the comparison with the ASTM[29] classification of coal rank, both BD and AB coals can be classified as high rank anthracitic coals. Hence, the main focus of this work will be the effect of burial depth and sampling location as well as the effect of sample size on the sorption behaviour of coals to CO_2 injection. As the distribution of structurally deformed coal within the northwest anthracite region of the South Wales coalfield is associated with areas of intense tectonically controlled shortening[8], it can be expected that the BD coal is more tectonically disturbed than the AB coal which is also visible in Figure 2 where BD core exhibits higher cleat density.

Table 1. Results of the coal characterization tests.

Characterization test	**BD**	**AB**
Proximate analysis		
Moisture content, %	1.65±0.12	0.91±0.3
Ash content, %	1.65±0.38	4.62±0.3
Volatile matter, %	5.82±0.21	5.73±0.08
Fixed carbon content, %	90.88	88.73
Ultimate analysis		
Total carbon content, %	90.12±0.11	89.5±0.66
Total sulphur content, %	0.95±0.02	0.87±0.04
Sulphur after full combustion content, %	-	0.25±0.05
Combustible sulphur content, %	-	0.62
Total hydrogen content, %	-	3.16±0.28
Nitrogen content, %	-	1.31±0.12
Oxygen content, %	-	0.33
Petrography		
Vitrinite reflectance, %	-	2.84±0.05
Vitrinite content, %	-	86.7
Liptinite content, %	-	0±1
Inertinite content, %	-	14±1
Mineral matter content, %	-	0±1
Calorimetry		

Higher calorific value, MJ/kg	-	33.6±0.22
Lower calorific value, MJ/kg	-	32.9

2.2.Experimental setup

Gas sorption experiments were conducted using a manometric sorption apparatus. The entire system has been designed to tolerate pressures up to 20 MPa and temperatures up to 338 K. The manometric unit was manufactured by GDS Instruments and contains two cells, each with a volume of 150 cm^3 separated by the needle valve (Figure 3a). On the top of each cell, a high pressure GDS transducer is mounted measuring up to 32 MPa with an accuracy of 0.15%. In order to maintain isothermal conditions during the experiments, the adsorption cell is submerged in a stainless-steel tank full of deionised water in which the temperature is controlled by a Thermo Haake temperature controller with an accuracy of 0.15%. A gas supply system consists of a liquid withdrawal carbon dioxide cylinder with 99% purity connected to a dual syringe Teledyne Isco 500D pump system (Figure 3b). Huber Pilot One Ministat 125 temperature controller, which circulates deionised water contained in a 2.75 L tank through the heating jackets mounted around the pumps, is used to maintain a constant temperature of a gas supply system. Before injecting any gas into the system, the adsorption cell and pipeline were vacuumed using a Bushi vacuum pump with a pressure of -0.09 MPa. For the helium pycnometry method, a stainless-steel calibration cell with a volume of 489.176 cm^3 was used. Total dead volume of the tubing system, valves and pressure transducers was 43.233 cm^3. A heater mat and a thermocouple were wrapped around the calibration cylinder to control the temperature of the gas inside it.

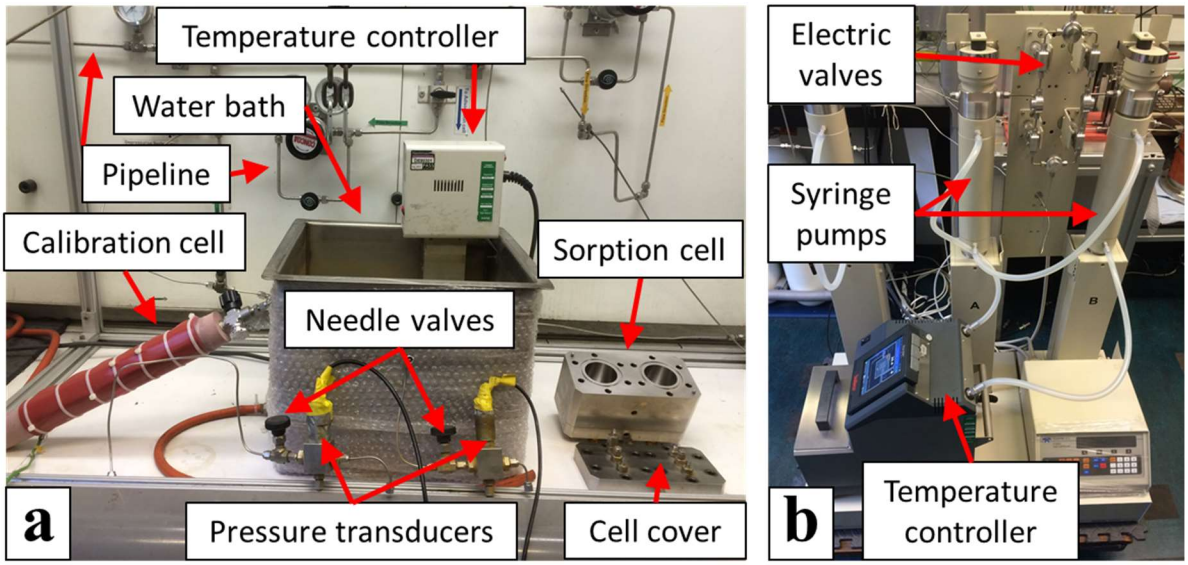

Figure 3. Images of the experimental units; a) Manometric sorption system, b) Syringe pumps.

2.3.Experimental conditions

Temperature of the manometric sorption system was maintained at 313.15±0.01K (40±0.01°C) enabling carbon dioxide to achieve its supercritical state at high pressures. Injection gas pressures up to 8.7 MPa were considered. It should be noted that pressure values mentioned in this study are absolute pressure values calculated assuming the atmospheric pressure of 101 325 Pa. If an average hydrostatic gradient of 0.01 MPa/m and an average thermal gradient of 0.03 K/m (°C/m) with an average surface temperature of 285K (12°C) are assumed, results of this study represent conditions existing up to approximately 900 m of depth.

2.4.Experimental procedure

In this work, the manometric sorption method was used which has been well documented previously in the literature[10, 11, 30-32], hence only brief details of steps undertaken in this investigation are provided in the following sections.

2.4.1. The Helium Pycnometry Method

Prior to the sorption experiment, the void volume of the sample cell containing a certain amount of coal was determined by expansion of helium under the assumption that the same pore volume is accessed by He as by CO_2 and that He does not adsorb on the coal surface[31]. Three measurements have been conducted for each tested sample where the average values of the calculated volumes for each cell have been used in sorption calculations. Before conducting the helium pycnometry method, all samples have been vacuumed for 24 hours. Such procedure removes the debris from the pores that would hinder the access of gas and also shrinks the pre-swollen coal matrix[33]. For the present work, this would include part of the residual moisture left there from the air-drying as well as any gases such as nitrogen and carbon dioxide that are a part of the ambient air, which might have adsorbed on the coal surface during the air-drying procedure.

2.4.2. Excess sorption measurements

In the manometric sorption measurement, defined amounts of gas are successively transferred from the reference cell into the sample cell containing the coal mass. Before the sorption process, coal samples were vacuumed for 2 hours to remove any residual helium. Experimental injection steps used in this study for coal samples of different sizes are presented in Table 2. In total, up to seven injection steps were applied for each coal sample. However, due to technical problems

encountered with the gas pressurising system and the pipeline, the last injection steps on 2.36-4.0 mm fractions could not have been conducted.

Table 2. Injection pressures used in the gas sorption measurements on coal samples of different sizes.

	Injection pressures in the reference cell (MPa)						
	1st step	2nd step	3rd step	4th step	5th step	6th step	7th step
Sample size	~0.6 MPa	~1.1 MPa	~2.6 MPa	~4.1 MPa	~5.6 MPa	~7.1 MPa	~8.6 MPa
BD							
0.25-0.85 mm	0.610±0.048	1.117±0.048	2.647±0.048	4.102±0.048	5.732±0.048	7.046±0.048	8.514±0.048
2.36-4 mm	0.629±0.048	1.100±0.048	2.650±0.048	4.107±0.048	5.700±0.048	7.149±0.048	-
Core	0.616±0.048	1.108±0.048	2.610±0.048	4.084±0.048	5.593±0.048	7.145±0.048	8.604±0.048
AB							
0.25-0.85 mm	0.620±0.048	1.140±0.048	2.595±0.048	4.121±0.048	5.482±0.048	7.244±0.048	8.718±0.048
2.36-4 mm	0.622±0.048	1.133±0.048	2.602±0.048	4.002±0.048	5.562±0.048	7.132±0.048	-
Core	0.633±0.048	1.136±0.048	2.595±0.048	4.136±0.048	5.597±0.048	7.105±0.048	8.588±0.048

The sorption equilibrium was considered to be reached when the pressure within the manometric sorption cell stabilized, i.e. when there was no change in the gas pressure. For powdered coal samples with 0.25-0.85 mm and 2.36-4 mm grain sizes, minimum time periods of 5 hours and 10 hours of a constant pressure were considered to mark the end of the sorption process, respectively. For core samples, a minimum time period of 20 hours of a constant pressure was considered. It should be noted that a maximum of twelve days of the equilibration time for each step was allowed. Although sorption of gases in coal is a slow process which can last up to two weeks for carbon dioxide[34], this value was chosen to minimize the risk of leakage and associated errors. The schematic setup for manometric sorption measurement is presented in Figure 4. The excess sorption was calculated directly from experimental quantities. The compressibility factors for CO_2 at different pressures were calculated applying the Span and Wagner[35] equation of state.

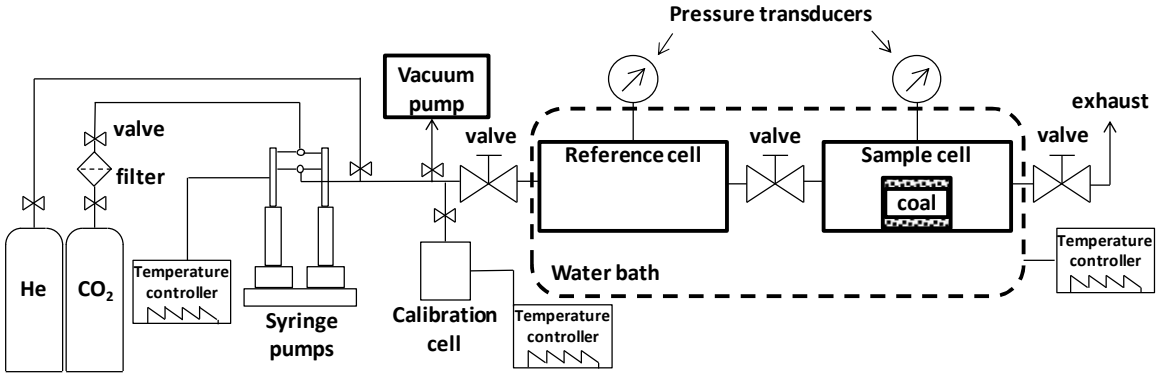

Figure 4. Schematic setup for the manometric sorption measurement.

2.4.3. Absolute sorption calculations

In the absolute sorption calculations, a commonly used value of 26.81 mmol/cm^3 (1180 kg/m^3) for the adsorbed phase density of CO_2 was selected from the literature[13, 15, 36]. Further confidence on the choice of the adsorbed phase density was based on the work of Gensterblum et al.[15] who estimated that the adsorbed phase density of CO_2 obtained on the Selar Cornish coal sample from the South Wales coalfield is 26.68±3.07 mmol/cm^3 (1174±135 kg/m^3), which corresponds to the density of the free phase at a pressure of 70.66 MPa at 318.58K.

The Langmuir equation[37] was used to fit the absolute sorption calculated. Although a range of sorption isotherms exists in the literature as discussed by White et al.[4], Langmuir curve offers good approximation for high-rank coals since such coals contain mainly micropores of nano-size[4, 38, 39]. Such pores are so small that they welcome only a couple of fluid molecules explaining why

Langmuir adsorption model provides good fit to the experimental data[40]. The absolute adsorbed amount n_L^{abs} (mol/kg) calculated via a Langmuir equation[37] is expressed as:

$$n_L^{abs} = n_L \frac{P_{eq}}{P_L + P_{eq}} \quad (1)$$

where P_{eq} is the equilibrium pressure (Pa), n_L and P_L are the Langumir parameters for the maximum sorption capacity (mol/kg) and the Langmuir pressure (Pa) at which coal achieves half of its maximum sorption, respectively.

In order to conduct the fitting procedure, the initial values were considered for the Langmuir parameters and the Langmuir absolute sorption was determined. Based on the experimental and fitted values of the absolute sorption, determination of the sum of the squared differences was conducted to minimize the residuals[12, 14]. The optimization procedure was performed using the Excel solver function by which the automatic adjustment, based on an iterative approach, of the Langmuir parameters to obtain the minimum value of the squared differences was performed.

2.4.4. Sorption kinetics calculations

To quantitatively present the pressure drop as a function of time recorded during every injection step, the pressure equilibration curves were normalized using an approach suggested previously[20]. In this approach the curves are expressed in terms of the residual or unoccupied sorption capacity, $Q_{residual}(t)$, calculated for each time interval as:

$$Q_{residual}(t) = \frac{n_t - n_{eq}}{n_{t(0)} - n_{eq}} \quad (2)$$

where, n_t, $n_{t(0)}$ and n_{eq} are the gas sorption amount at time t (h), the initial gas sorption at the beginning of each pressure step and the total gas sorption at equilibrium, respectively.

Calculated residual sorption capacity values were then analysed based on the first-order rate function, second-order rate function and semi-empirical equation proposed by Busch et al.[20].

The integrated representation of the first rate-order function can be expressed as:

$$Q_{residual}(t) = Q_{residual\,(0)} \cdot e^{-k\,t} \quad (3)$$

where, $Q_{residual\,(0)}$ is the initial residual sorption at the start of the time step and k is the first-order reaction rate (s^{-1}).

The second-order rate function, in its integrated form, can be presented as:

$$\frac{1}{Q_{residual}(t)} = \frac{1}{Q_{residual\,(0)}} + k't \quad (4)$$

where k' is the second-order reaction rate (s^{-1}).

Busch et al.[20] expressed the amount of the residual capacity by the combined first-order rate function as:

$$Q_{residual}(t) = Q_1 \cdot e^{-k''\,t} + Q_2 \cdot e^{-k'''\,t} \quad (5)$$

where Q_1 and Q_2 are the residual sorption capacities with $Q_1 = 1 - Q_2$, where $0 \leq Q_1 \leq 1$, and k'' and k''' are the two first-order reaction rates (s^{-1}).

3. Results

3.1.Experimental pressure decay curves

Experimental results of the manometric sorption measurements on BD and AB coal samples are presented in Figures 5 and 6, respectively. Each figure shows the pressure measured as a function of time at each injection step for three samples of different sizes, i.e. powdered coal samples with grain sizes of 0.25-0.85 mm and 2.36-4 mm, and coal cores.

The results show that for the first three injection pressures considered, the sorption time is up to maximum 250 hours for the AB coal and 80 hours for the BD coal. During subsequent injection steps, the equilibrium time reduces to maximum 50 hours and 120 hours for BD and AB samples, respectively. If the behavior of BD and AB samples is compared in more detail, pressure decay curves for both coals reveal that sorption behavior is grain size dependent, where equilibrium time increases with an increase in grain size. The average equilibrium time for samples with grain size of 0.25-0.85 mm from both coals (BD and AB) was up to 8 hours and shapes of the pressure decay curves for each pressure step of both coals are comparable. Samples with grain size of 2.36-4 mm show different behaviour. The BD sample required up to 45 hours to reach equilibrium, while the AB sample required longer time, i.e. up to 60 hours. The difference in the equilibration time is even more pronounced between the core samples. Experimental data for the BD core show the equilibration time up to 80 hours while the AB core took more than 3 times longer to complete the sorption process at each injection step, i.e. up to 250 hours. This demonstrates that higher cleat density in the BD core enabled faster adsorption rates than in the AB core.

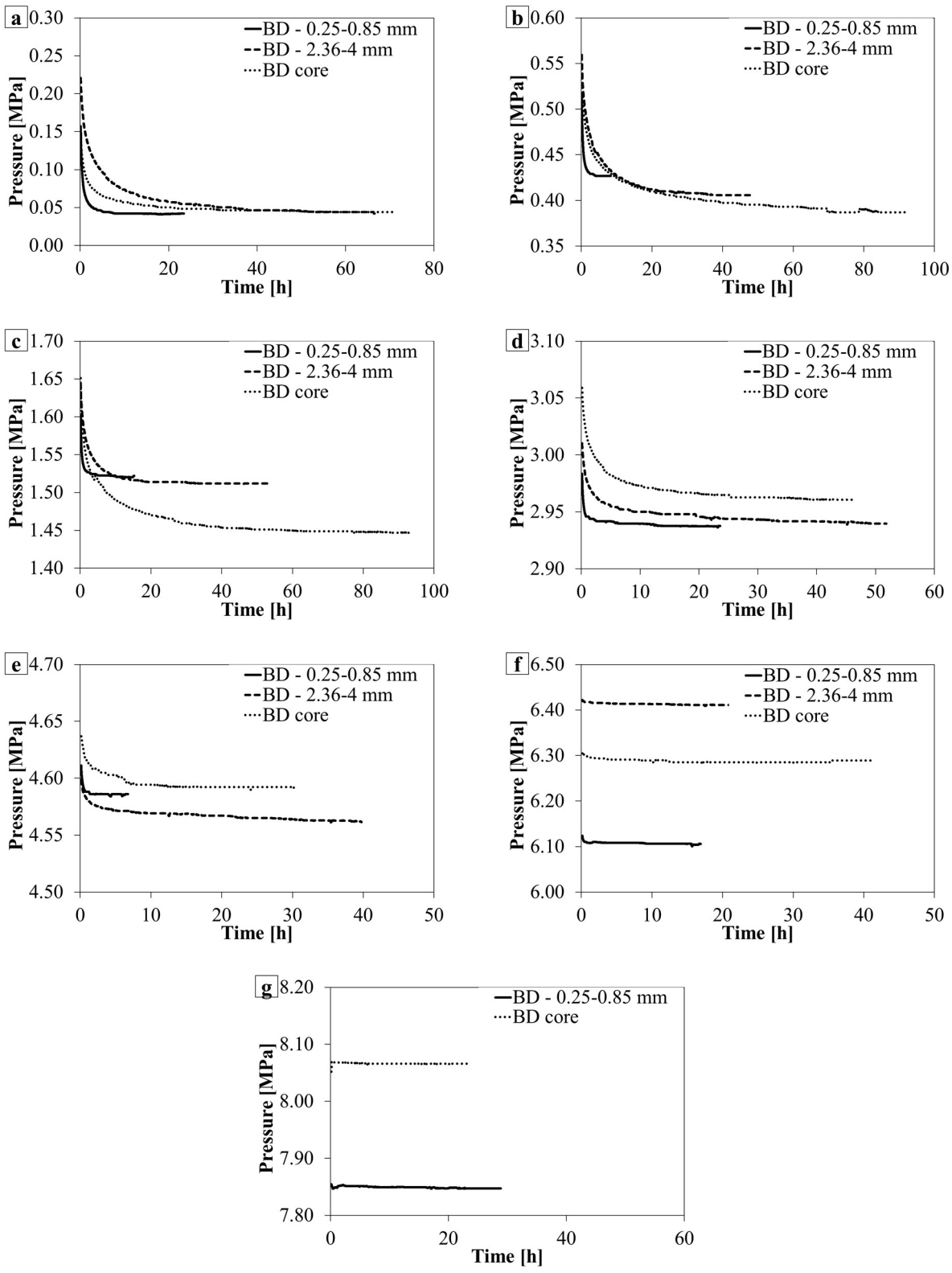

Figure 5. Pressure decay curves for three BD coal samples of different sizes at various injection pressures; a) 1st step, b) 2nd step, c) 3rd step, d) 4th step, e) 5th step, f) 6th step, g) 7th step.

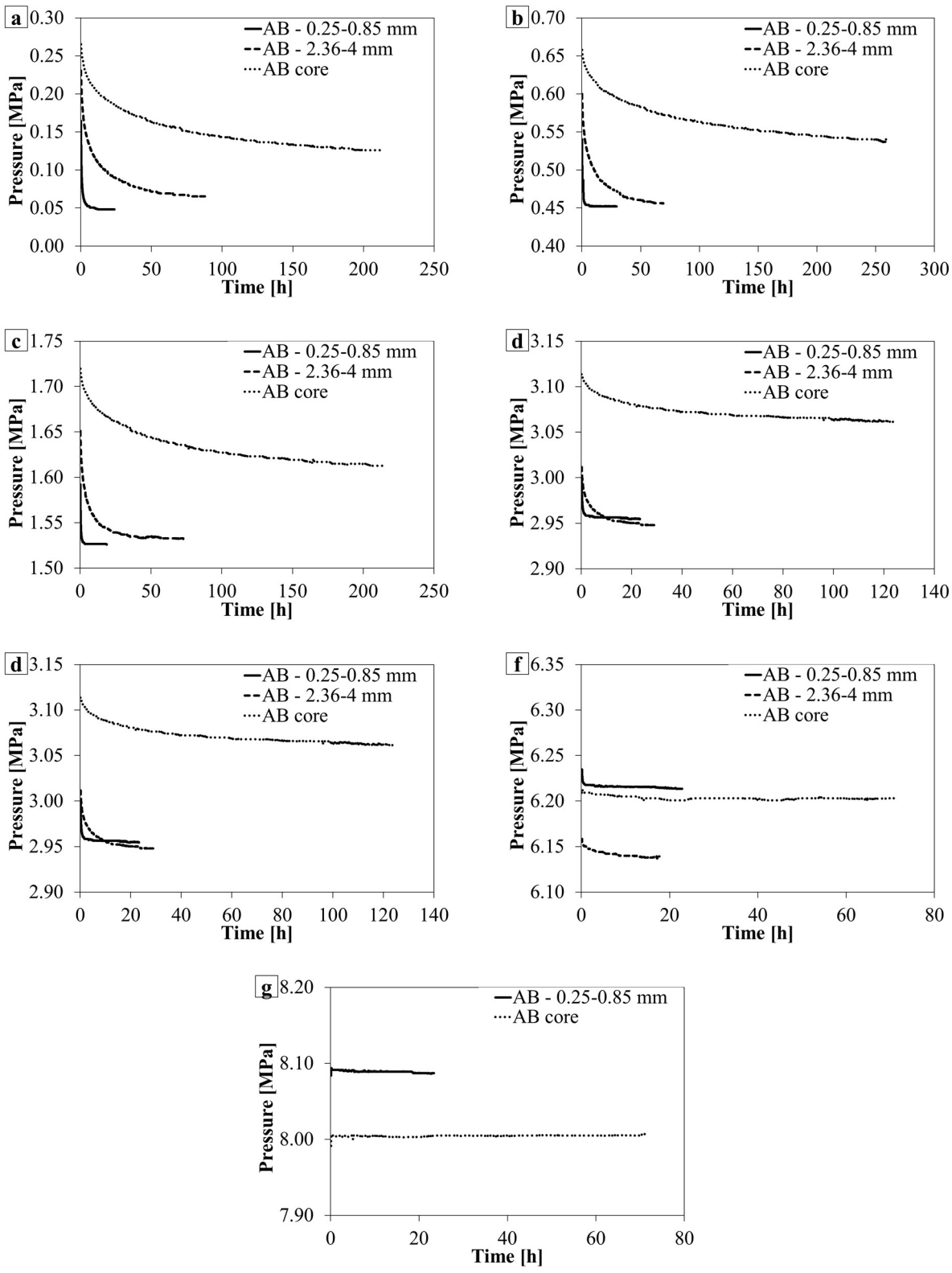

Figure 6. Pressure decay curves for three AB coal samples of different sizes at various injection pressures; a) 1st step, b) 2nd step, c) 3rd step, d) 4th step, e) 5th step, f) 6th step, g) 7th step.

3.2.Excess sorption

Excess sorption isotherms for all three samples of different sizes from both BD and AB coals are presented in Figure 7. As shown for both BD and AB coal samples, the amount of excess sorption increases gradually with an increase in gas pressure up to 5 MPa and then decreases with further increase in gas pressure. Such behaviour is attributed to the experimental determination of the excess sorption where the volume of the adsorbed phase is neglected.

For the 0.25-0.85 mm grains, the maximum excess sorption amounts calculated at 4.7 MPa and 4.5 MPa of BD and AB coals are 1.63 mol/kg and 1.5 mol/kg, respectively. This shows that the maximum excess sorption capacity of the AB coal is 8% less than of the BD coal. Results presented for the 2.36-4 mm grains calculated at 4.6 MPa show that the maximum sorbed amount of 1.42 mol/kg for the AB coal is 13% lower than the maximum excess sorption of 1.64 mol/kg for the BD coal. The maximum excess sorption values of BD and AB cores calculated at 6.4 MPa and 6.3 MPa are 1.49 mol/kg and 0.75 mol/kg, respectively. This shows that AB coal core has 50% lower excess sorption capacity compared to the BD core.

By comparing the maximum excess sorption capacity reported above between the samples of different sizes of the BD coal, the difference between the 0.25-0.85 mm and 2.36-4.0 fractions is less than 1% which is within the error range of the measurement system, as will be shown in the following section. The maximum excess sorption capacity of the BD core is 9% less than of the powdered BD samples. The 0.25-0.85 mm fraction of the AB coal shows 6% and 50% higher maximum sorption capacity than the 2.36-4.0 mm and AB core, respectively.

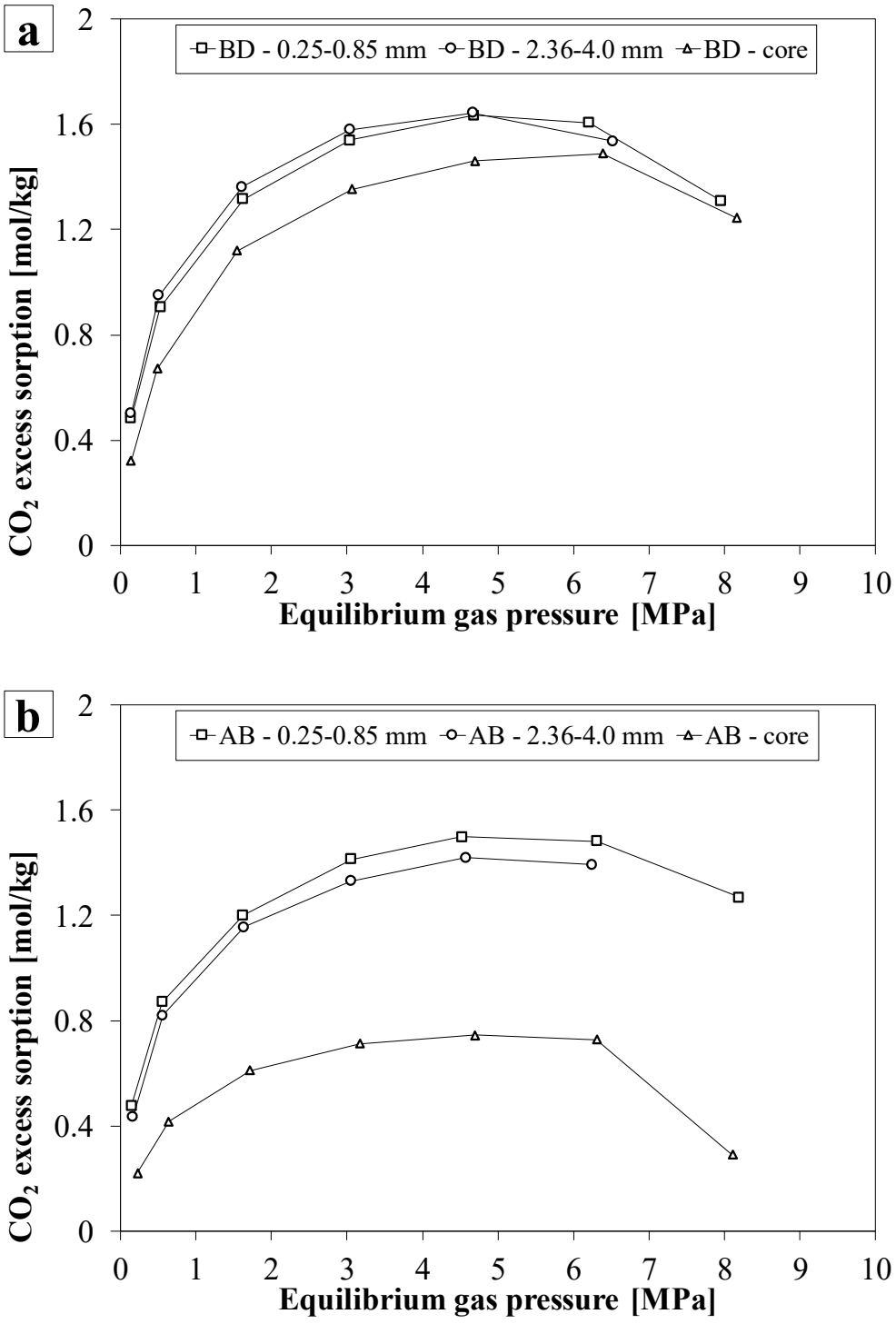

Figure 7. Excess sorption of CO_2 on coal samples of different sizes; a) BD coal, b) AB coal.

3.2.1. Error analysis

In this section, an error analysis is conducted to estimate the accuracy of an excess adsorption determination based on the experimental error of the measurement system. As explained earlier, pressure in the manometric sorption apparatus is the main variable measured in all the experiments, i.e. helium pycnometry and adsorption measurements. The error in temperature is considered to be negligible in this work due to the high accuracy of the temperature control system. Furthermore, Busch and Gensterblum[32] have shown that temperature change of 0.1K causes an error only up to 0.005 mol/kg for the range of pressures considered in this study. Hence, the uncertainty in the experimental results related to the accuracy of the pressure transducers is analysed. A value of ±48 kPa is taken for calculations representing accuracy of 0.15% of full range output of 32 MPa pressure transducer. The errors in the amounts adsorbed related to the uncertainty in the pressure readings during the determination of the void volumes of the reference and sample cells are given in Table 3. In addition, the errors in the amounts of CO_2 injected and adsorbed associated with the uncertainty in the pressure readings during the CO_2 adsorption experiments are shown in the same table.

Table 3. Error analysis of excess sorption values associated with an experimental uncertainty during pressure readings.

	BD 0.25-0.85 mm		BD 2.36-4.0 mm		BD core		AB 0.25-0.85 mm		AB 2.36-4.0 mm		AB core	
Injection steps	**Positive error value (mol/kg)**	**Negative error value (mol/kg)**	**Positive error value (mol/kg)**	**Negative error value (mol/kg)**	**Positive error value (mol/kg)**	**Negative error value (mol/kg)**	**Positive error value (mol/kg)**	**Negative error value (mol/kg)**	**Positive error value (mol/kg)**	**Negative error value (mol/kg)**	**Positive error value (mol/kg)**	**Negative error value (mol/kg)**
Error in excess sorption values due to pressure readings (±48 kPa) during determination of void volumes of the reference and sample cells using He												
1st step	0.011	0.010	0.011	0.010	0.007	0.007	0.010	0.009	0.009	0.008	0.004	0.004
2nd step	0.017	0.016	0.018	0.017	0.014	0.013	0.015	0.014	0.013	0.013	0.006	0.006
3rd step	0.012	0.013	0.013	0.014	0.018	0.018	0.009	0.010	0.008	0.009	0.002	0.003
4th step	0.002	0.005	0.001	0.004	0.014	0.014	0.004	0.007	0.006	0.008	0.007	0.008
5th step	0.029	0.035	0.027	0.033	0.002	0.004	0.026	0.031	0.028	0.033	0.021	0.025
6th step	0.066	0.077	0.087	0.099	0.014	0.017	0.066	0.075	0.064	0.074	0.044	0.049
7th step	0.151	0.172	-	-	0.058	0.066	0.157	0.176	-	-	0.102	0.114
Error in excess sorption values due to pressure readings (±48 kPa) during the CO_2 injection												
1st step	0.047	0.048	0.047	0.047	0.024	0.024	0.047	0.047	0.047	0.047	0.029	0.029
2nd step	0.045	0.045	0.045	0.045	0.022	0.022	0.045	0.045	0.045	0.045	0.028	0.028
3rd step	0.042	0.042	0.042	0.042	0.019	0.019	0.042	0.042	0.042	0.042	0.027	0.027
4th step	0.038	0.038	0.038	0.038	0.016	0.016	0.038	0.038	0.038	0.038	0.024	0.024
5th step	0.029	0.028	0.029	0.029	0.011	0.011	0.031	0.031	0.031	0.030	0.020	0.020
6th step	0.007	0.005	0.009	0.008	0.005	0.004	0.003	0.000	0.005	0.003	0.005	0.003
7th step	0.213	0.187	-	-	0.125	0.114	0.233	0.237	-	-	0.132	0.118

As evident from Table 3, errors in the pressure readings during the determination of the void volumes of the cells can yield errors in the amounts adsorbed. The errors determined show an increase with the injection step applied, i.e. CO_2 pressure, with the maximum error in the subcritical region up to 0.08 mol/kg, 0.1 mol/kg, 0.02 mol/kg for BD coal and 0.08 mol/kg, 0.07 mol/kg, 0.05 mol/kg for AB coal determined on 0.25-0.85 mm, 2.36-4.0 mm and core samples, respectively. The highest errors are obtained in the supercritical region, up to 0.17 mol/kg for the 0.25-0.85 mm fractions on both coals. The errors in the supercritical region for BD and AB cores are up to 0.07 mol/kg and 0.11 mol/kg. The errors in the amounts of CO_2 injected and adsorbed associated with the pressure readings during the CO_2 adsorption experiments can yield errors up to 0.05 mol/kg in the subcritical range for all samples. Errors are the highest in the supercritical region, up to 0.24 mol/kg for the 0.25-0.85 mm samples and 0.13 mol/kg for the cores. Larger errors obtained for measurements on the powdered samples compared to the cores are due to the larger ratio of void volume to the coal mass used, i.e. packing more coal into the sample cell minimizes the effect of the void volume size[31]. These findings on the effects of experimental uncertainties on the adsorption values are consistent with the ones reported in the literature[10, 31, 32].

3.3.Absolute sorption

Figure 8 presents the absolute sorption isotherms fitted to the calculated absolute adsorption values obtained on samples of different sizes from BD and AB coals. From the results presented, it can be seen that fitting the Langmuir curve to the absolute adsorption capacity determined experimentally shows very good agreement. However, a difference of 0.33 mol/kg between the calculated and fitted values for AB core at CO_2 pressure of 8.1 MPa (Figure 7b) could be related to the experimental uncertainty. Furthermore, as suggested previously[11, 41], the volume occupied by CO_2 may not by the same at high pressures as in the low-pressure region, as swelling of the

coal matrix may restrict the access to pores and increase the volume of the solid adsorbent affecting the calculated sorption capacity.

It can be observed from Figure 8 that the amount of absolute sorption continuously increases with gas pressure. If the absolute sorption isotherms of three samples of different sizes between the BD and AB coals are compared, it can be noticed that BD samples show higher sorption capacity over the pressure range considered than AB samples.

In particular, if the absolute sorption data presented for 0.25-0.85 mm grains in Figure 8a (BD) and Figure 8b (AB) are compared, it can be observed that the absolute sorption capacity values of the BD and AB samples at approximately 6.3 MPa are 1.85 and 1.72 mol/kg, respectively. Hence, the sorption capacity of the AB coal is 7% lower than that of the BD coal. For grains with size of 2.36-4 mm, the absolute sorption capacity values at 6.5 MPa are 1.80 mol/kg (BD) and 1.61 mol/kg (AB) showing a difference of 11%. The presented data for the cores reveal two times higher sorption for BD in comparison to AB coal. In particular, BD and AB cores show absolute sorption capacities of 1.73 mol/kg and 0.85 mol/kg at 6.4 MPa, respectively. Therefore, as the sample size increases, the difference in absolute sorption capacities between the BD and AB coals also increases.

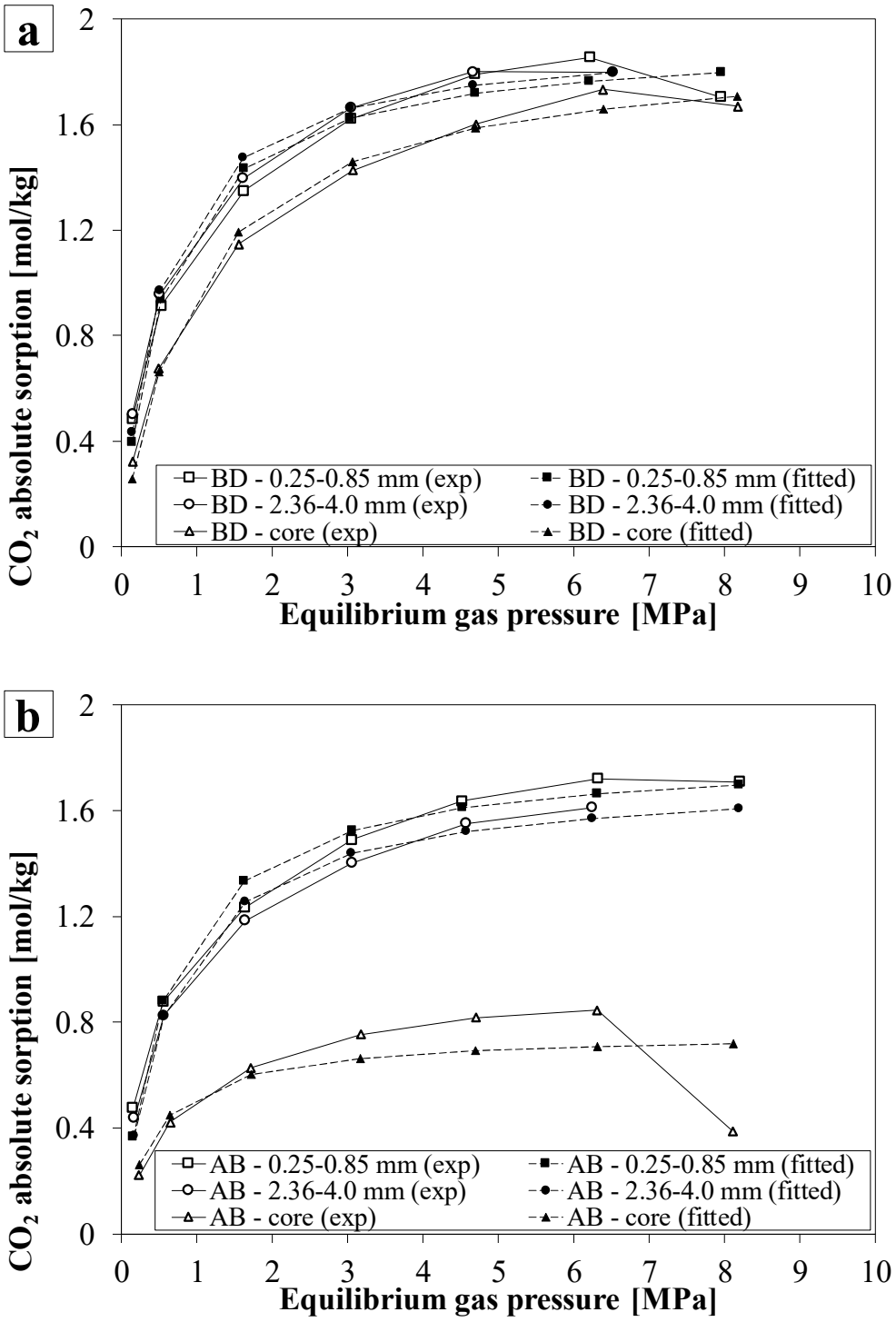

Figure 8. The CO_2 absolute sorption isotherms fitted to the calculated absolute sorption values on coal samples of different sizes; a) BD coal, b) AB coal.

Figure 9 presents the fitted parameters for the absolute gas sorption on all the samples of both coals. According to the results, maximum absolute sorption capacity values of the BD samples with grain sizes of 0.25-0.85 mm, 2.36-4 mm and core are 1.92 mol/kg, 1.94 mol/kg, and 1.9 mol/kg, respectively (Figure 9a). Results for the AB coal show maximum absolute sorption capacity values of 1.82 mol/kg, 1.73 mol/kg, and 0.75 mol/kg for 0.25-0.85 mm grains, 2.36-4 mm grains and core, respectively. Therefore, BD coal shows only up to 2 % difference in the maximum sorption capacities between the powdered and core samples, which is within the error margins of the experimental system demonstrating that the maximum sorption capacity of all BD coals is the same, irrespective of the sample size. However, such difference is more pronounced for the AB coal, yielding a drop of 5% and 59% of sorption capacities for 2.36-4.0 mm grains and AB core in comparison to the 0.25-0.85 mm grains, respectively.

As shown in Figure 9b, the pressures at which half of the maximum sorption has been achieved varies between 0.51 and 0.91 MPa for the BD coal and between 0.44 and 0.61 MPa for the AB coal. This indicates that half of the CO_2 sorption on anthracite samples occurs at low pressures, i.e. <1.0 MPa.

Previously reported results on high-rank coals from different locations of the South Wales coalfield for crushed samples with grain diameter of <2 mm obtained at 318K are 1.8 mol/kg and 1.92 mol/kg[15, 42]. Both values are in close agreement with the reported values for 0.25-0.85 mm and 2.36-4.0 mm fractions of AB and BD samples as well as the BD core of this study but differ up to 61% from the results obtained on AB core.

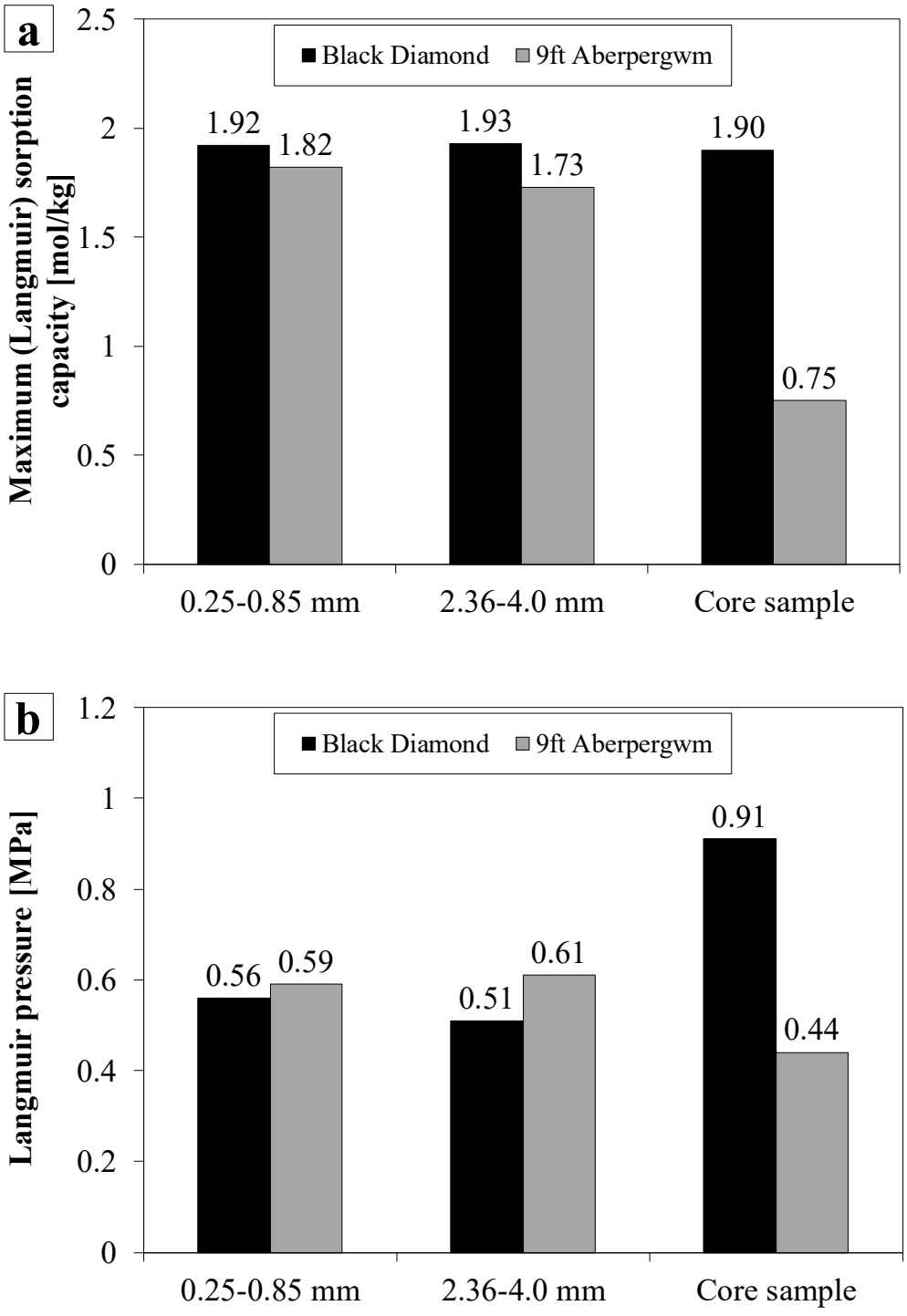

Figure 9. Fitted Langmuir parameters for the absolute CO_2 sorption capacity of all the measured samples; a) Maximum (Langmuir) sorption capacity, b) Langmuir pressure.

3.4.Sorption kinetics

Figure 10 presents the results of residual gas sorption capacity with respect to time calculated using the equation (2) for all samples. However, in order to study the kinetic effect of the CO_2 sorption process in coal, the last two injection steps were disregarded. Reasons for that are the short time of equilibration and low-resolution data as a result of small amount of gas adsorbed. In addition, each figure contains three approaches to match experimental pressure decay curves calculated using equations (3) to (5).

Constants related to the first-order, second-order and two combined first-order rate equations were obtained by fitting the models to the experimental results. A summary of the parameters obtained is given in Table 4. Based on the fitting parameters obtained, i.e. sorption rate constants, it can be observed that values of constants decrease with an increase in sample size up to 2.36-4.0 mm for both coals. In particular, up to 10 and 17 times higher sorption rates are observed in 0.25-0.85 mm samples compared to 2.36-4.0 mm samples in BD and AB coals, respectively. However, the reduction of the fitting parameters with further increase in sample size is only observable for the AB coal, reducing by a factor of more than 100 between the 0.25-0.85 mm and core samples. The 0.25-0.85 mm samples of both coals showed very similar sorption rate constants, i.e. maximum differences up to 6% and 3% in constants obtained using first-order and second-order functions, respectively. The differences between the sorption rate constants obtained on larger samples of BD and AB coals were more pronounced, i.e. between 45% and 92%.

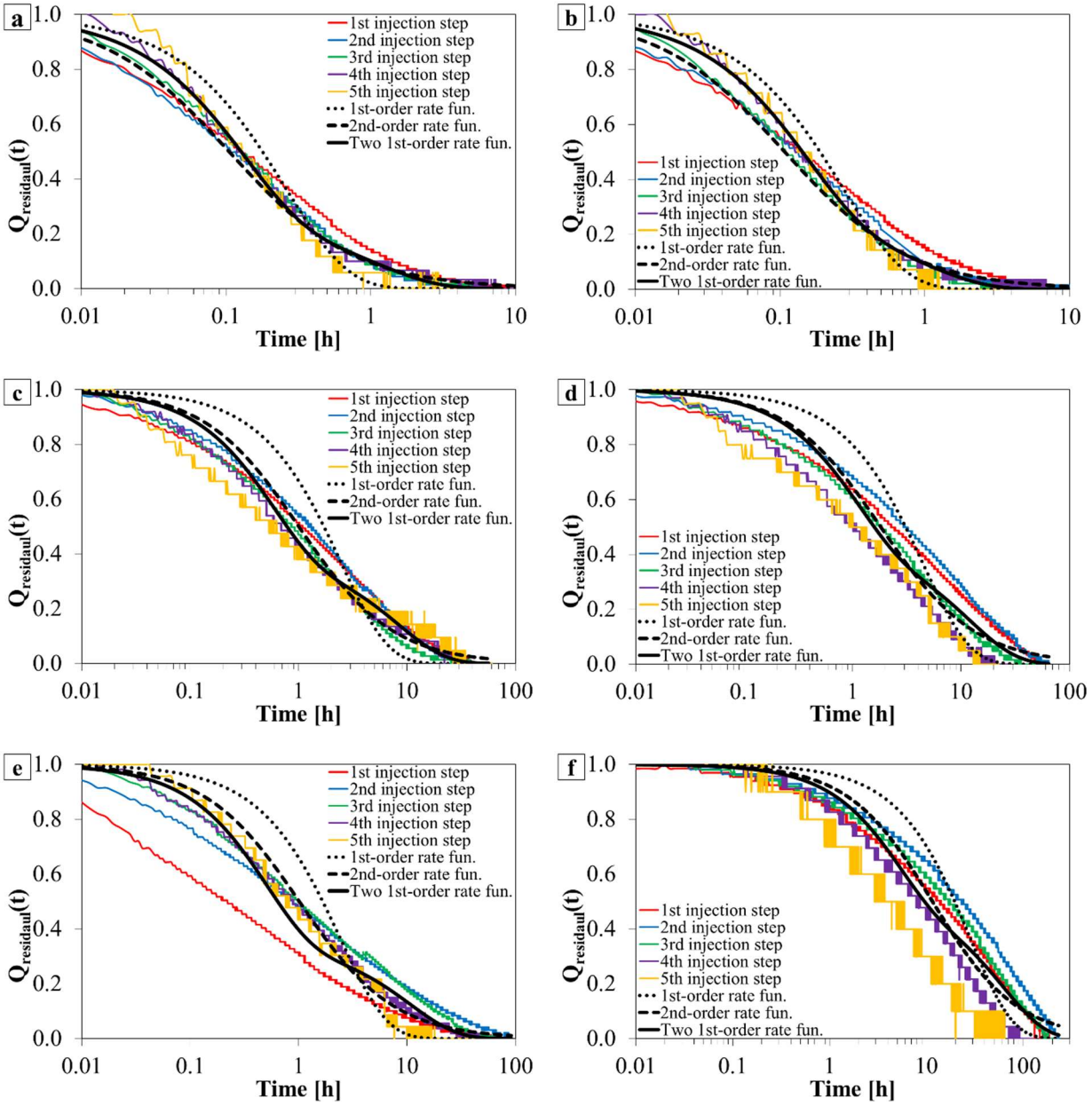

Figure 10. The fits of the experimental residual capacity decline: a) BD 0.25-0.85 mm, b) AB 0.25-0.85 mm, c) BD 2.36-4.0 mm, d) AB 2.36-4.0 mm, e) BD core, f) AB core.

Table 4. Summary of the sorption rate constants obtained from the 1st order, 2nd order and two combined 1st order sorption kinetics models.

Grain size	First-order	Second-order	Two first-order			
	k (h^{-1})	k' (h^{-1})	k'' (h^{-1})	k''' (h^{-1})	Q_1	Q_2
BD coal						
0.25-0.85 mm	3.88	9.52	7.89	0.93	0.75	0.25
2.36-4.00 mm	0.41	1.00	1.82	0.12	0.61	0.39
Coal core	0.42	0.99	2.04	0.094	0.66	0.34
AB coal						
0.25-0.85 mm	3.66	9.25	6.85	1.01	0.74	0.26
2.36-4.00 mm	0.23	0.55	0.082	0.98	0.43	0.57
Coal core	0.035	0.086	0.016	0.21	0.51	0.49

4. Discussion

4.1. Effect of sample size

Overall, the total carbon dioxide sorption on the smallest coal grains (0.25-0.85 mm) from both BD and AB coals was completed within one week, while experiments on the 2.36-4 mm grains lasted up to two weeks each. Cores from BD and AB coals took the longest time to finish the sorption process, two and a half weeks and six weeks, respectively (Figures 5 and 6).

Although sorption is a phenomenon predominantly occurring at a surface of the coal, the time taken to reach equilibrium in a pressure step is dependent on several factors. Both the time taken for the molecules to arrive at the adsorption sites within the coal grains and the time required for molecules to physically or chemically interact with the coal surface upon contact must be considered. As larger samples provide higher sorption area, the sorption time can increase as a consequence.

By inspecting the adsorption rate constants (Table 4 and Figure 10), the rate of adsorption in BD samples decreases with an increase in sample size up to 2.36-4.0 mm above which, the adsorption rates remain relatively constant. The fastest sorption in the smallest particles, i.e. 0.25-0.85 mm, is associated with the fact that powdered samples loose most of their macropores (> 50 nm) and the fracture network during the crushing process[25]. In addition, for the grain size of 0.25-0.85 mm, it can also be expected that due to the powdering process and very small grain sizes as a result, previously restricted and dead-end pores might be opened leading to easier accessibility of the sorption sites resulting in fast adsorption process. Hence, the adsorbed amount and time associated with the sorption on the smallest samples is attributed predominantly to the pore filling and CO_2 dissolution in the coal matrix due to the high exposure of pores to the gas. Larger samples, i.e. 2.36-4.0 mm and core, additionally include transport mechanisms within the cleat system, mass exchange between the fractures and the matrix as well as the diffusion of gas molecules within the microporous system to the sorption sites.

With respect to the sorption isotherms (Figures 8 and 9), the change of maximum sorption capacity with an increase in BD sample size is negligible. Such behaviour is attributed to the interconnectivity of the fracture network and the distance between the fractures in the BD core. In particular, well-developed cleat system in the BD core (Figure 2b) and short distances between the cleats allowed easy access to the microporous matrix for the CO_2 molecules which resulted in a sorption capacity equal to the one determined on powdered BD samples.

The sorption capacity and kinetics of sorption on the AB coal showed different behavior, i.e. the sorption response of AB coal shows a decrease with an increase in the sample size, with the most significant change between 2.36-4.0 mm particles and the core. These observations are opposite to the ones reported by Pone et al.[19] who have observed that at gas pressure of 3.1 MPa, unconfined

bituminous coal core sorbed 1.4 mol/kg in comparison to 1.2 mol/kg sorbed by powdered samples. Pone et al.[19] assumed that this might be an indication that pulverization of coal generates new pores or that dispersion of lithotypes in crushed samples is different than the ones originally in banded coals. However, more recently, Staib et al.[25] have demonstrated that crushing of the coal increased the total porosity of the sample accessible to gas. Hence, the newly accessible pores as a result of finer grinding offered more sorption sites and consequently, increased the sorption capacity in crushed AB samples compared to the AB core with low cleat density in which the access to the micro-pores is limited lowering the sorption capacity as a consequence.

Due to the high exposure of sorption sites to CO_2 in all BD samples, i.e. powdered and core, and powdered AB samples, more than 80% of the total sorption occurred in the early stage of each pressure step, i.e. up to the first 10 hours, with the remainder of the sorption occurring at the subsequent slower stage (Figure 9). Katyal et al.[39] concluded that large samples with poor fracture network have a structure highly constricted by ultra micropores (< 0.6 nm) in which the sorption is marked by the slow rates. As the AB core does not show a great extent of fracturing which would enable easy access for the CO_2 molecules to the microporous matrix and sorption sites, it exhibited a behaviour where sorption occurred more gradually in each pressure step as a result, with 50% of the total sorption within the first 10 hours.

4.2.Effect of coal location and burial depth

Although both coals are of the same rank and belong to the same coal seam, i.e. 9ft seam, the complexity and extent of the cleats in the BD coal facilitated faster penetration of gas into the coal and easier access to the coal matrix and sorption sites as explained earlier. The cause of this difference can be related to the location of the BD and AB coals within the South Wales coalfield.

The structure and deformation of the coalfield has been extensively discussed in the literature[8, 43, 44] and it was concluded that coal seams in the South Wales coalfield responded in a highly brittle manner to deformation which increased the fracture frequency and decreased the strength and average size of the coal products. In the South Wales anthracites the level of deformation was the greatest in the northwest of the coalfield comprising the highest coal rank[8]. As a result of such deformation associated changes, the fracture systems characterized by feather and slickenside macrofractures and related micro-fractures were developed making anthracites more friable as a result of close cleat spacing[8]. In particular, the East Pit mine where the BD coal was provided from, has been recorded to contain seams with slip planes relatively closely spaced, i.e. more than five per meter, producing a coal product abnormal in appearance and structurally weakened[44, 45].

Another potential reason for the difference in lower sorption capacity of the AB samples compared to the BD samples is the ash content of the coals. As shown in Table 1, ash content of the AB coal is approximately three times higher than of the BD coal. The sorption capacity of coal for CO_2 decreases with an increase in ash content, and organic matter controls the storage capacity of coals[32]. Furthermore, coals with higher ash content tend to have larger cleat spacing than coals with low ash content[6].

Source of the variation in the sorption behaviour caused by different fracture interconnectivity of the two coals is also associated with the depths of the coal seams, i.e. BD was obtained from 150 m and AB from 550 m depth. As suggested previously[6], deeper coal seams may have less developed fracture network as a result of geological effects. Deeper coal seams may be more affected by the tectonism which might obliterate previously formed cleats[6]. In addition, butt cleats which connect one face cleat to another may be in some cases only restricted to near-surface locations which will clearly impact interpretation of fracture connectivity in coal beds at depth[6].

In particular, at shallower depths uplift and erosion increase driving stress for fracture propagation where pre-existing face cleats tend to relieve induced stresses perpendicular to them and inhibit growth of additional parallel fractures[6].

5. Conclusions

This paper presented the experimental results of CO_2 sorption measurements on coal samples of various sizes (0.25-0.85 mm, 2.36-4 mm and cores), obtained from the same coal seam but from different locations and depths of the South Wales Coalfield. BD coal was obtained from 150 m depth of an opencast coal mine 16 km away from an underground mine where AB coal was extracted from 550 m depth. The main conclusions of this work can be summarized as follows:

- High-rank coal samples from the South Wales coalfield (UK) considered in this study showed a significant potential for storage of CO_2, with maximum adsorption capacities up to 1.93 mol/kg (BD coal) and 1.82 mol/kg (AB coal).
- BD coal showed higher sorption capacity than the AB coal and the difference between the sorption capacities increases with an increase in the sample size. The largest difference of 58% was found to be between the core samples and the smallest difference of 5% between the powdered samples with grain size 0.25-0.85 mm.
- The differences in the sorption behaviour were mainly related to the cleat structure each coal exhibits which was associated with burial depths and sampling locations of each coal. As the BD coal comes from an area of the coalfield more affected by deformation and erosion than the AB coal, higher cleat density observed in BD coal enabled easier access of the CO_2 molecules to the sorption sites. Different ash contents of the coals were also associated with differences in the sorption behaviour.

- An increase in sample size did not affect the sorption capacity of BD coal, however it decreased the sorption rates between the 0.25-0.85 mm and 2.36-4.0 mm samples. The difference in sorption rates between 2.36-4.0 mm and core samples was negligible leading to the conclusion that in large particles with well-developed fracture network, transport along the cleats is a controlling factor while the inter-cleat diffusion distances remain essentially constant.
- Both the sorption capacity and kinetics of sorption determined on AB coal were dependent on the grain size, with a significant decrease in sorption parameters determined on the AB core compared to powdered samples associated with low cleat density which hindered the access of CO_2 molecules to the sorption sites. This indicated that grinding of coals increases the total porosity accessible to gases and allows quicker access of gas molecules to the sorption sites which might not reflect the behavior of large intact coal samples with low cleat density.
- Both BD and AB coals achieved more than half of their maximum CO_2 adsorption capacity at pressures below 1 MPa demonstrating a significant storage potential whereas majority of the CO_2 can be stored in its subcritical state.

Overall, this study demonstrated the CO_2 sequestration potential of anthracite coals, especially within the South Wales coalfield known for its deformation associated changes in fracture frequency and appearance of coal. Hence, to conduct a successful carbon sequestration project, a comprehensive geological assessment of the CO_2 storage target area is required to identify deformation induced fracture systems. If a well-developed cleat network, which can allow accessibility of gases to sorption sites, is identified at target high-rank coal bearing locations, such coals can be considered as an option for CO_2 sequestration. Where the high-rank coal seams have

wide cleat spacing which can increase the amount of time required for the diffusing gas to reach the sorption sites affecting the injectivity and economics of the project, inducement of new fractures and enhanced propagation of the existing ones through stimulation techniques could facilitate the sorption of CO_2 by decreasing the mean diffusion distance from the pores to a permeability conduit.

AUTHOR INFORMATION

Corresponding Author

*Renato Zagorscak, email: ZagorscakR@cardiff.ac.uk

Author Contributions

The manuscript was written through contributions of all authors. All authors have given approval to the final version of the manuscript.

ACKNOWLEDGMENT

This work was carried out as a part of SEREN and FLEXIS Projects. Both projects have been part-funded by the European Regional Development Fund through the Welsh Government. The financial support, for the first author, is gratefully acknowledged. The authors wish to express their appreciation to EnergyBuild Ltd., Walter Energy Inc. and Celtic Energy Ltd. for providing coal blocks to conduct this research.

ABBREVIATIONS

AB, Aberpergwm coal; ASTM, American Society for Testing and Materials; BD, Black Diamond coal; CCS, Carbon Capture and Storage.

REFERENCES

1. The Intergovernmental Panel on Climate Change (IPCC), *Global warming of 1.5°C. An IPCC Special Report on the impacts of global warming of 1.5°C above pre-industrial levels and related global greenhouse gas emission pathways, in the context of strengthening the global response to the threat of climate change, sustainable development, and efforts to eradicate poverty* (2018).
2. The Royal Society and Royal Academy of Engineering, *Greenhouse gas removal.* Report, (2018).
3. International Energy Agency (IEA). *Carbon Capture and Storage: The solution for deep emissions reductions*. IEA, (2015).
4. White, C.M., et al., *Sequestration of carbon dioxide in coal with enhanced coalbed methane recovery a review.* Energy & Fuels, **19**(3): p. 659-724, (2005).
5. Clarkson, C. and R. Bustin, *The effect of pore structure and gas pressure upon the transport properties of coal: a laboratory and modeling study. 1. Isotherms and pore volume distributions.* Fuel, **78**(11): p. 1333-1344, (1999).
6. Laubach, S.E., Marrett, R.A., Olson, J.E. and Scott, A.R., *Characteristics and origins of coal cleat: A review.* International Journal of Coal Geology, **35**(1-4): p. 175-207, (1998).
7. Moore, T.A., *Coalbed methane: a review.* International Journal of Coal Geology, **101**: p. 36-81, (2012).
8. Harris, I.H., G.A. Davies, R.A. Gayer, and K. Williams, *Enhanced methane desorption characteristics from South Wales anthracites affected by tectonically induced fracture sets.* Geological Society, London, Special Publications, **109**(1): p. 181-196, (1996).
9. Sakurovs, R., S. Day, S. Weir, and G. Duffy, *Application of a modified Dubinin− Radushkevich equation to adsorption of gases by coals under supercritical conditions.* Energy & fuels, **21**(2): p. 992-997, (2007).
10. Krooss, B.v., F. Van Bergen, Y. Gensterblum, N. Siemons, H. Pagnier, and P. David, *High-pressure methane and carbon dioxide adsorption on dry and moisture-equilibrated Pennsylvanian coals.* International Journal of Coal Geology, **51**(2): p. 69-92, (2002).
11. Ozdemir, E., B.I. Morsi, and K. Schroeder, *CO2 adsorption capacity of argonne premium coals.* Fuel, **83**(7-8): p. 1085-1094, (2004).
12. Bae, J.-S. and S.K. Bhatia, *High-pressure adsorption of methane and carbon dioxide on coal.* Energy & Fuels, **20**(6): p. 2599-2607, (2006).
13. Goodman, A., et al., *Inter-laboratory comparison II: CO2 isotherms measured on moisture-equilibrated Argonne premium coals at 55 C and up to 15 MPa.* International Journal of Coal Geology, **72**(3-4): p. 153-164, (2007).

14. Siemons, N. and A. Busch, *Measurement and interpretation of supercritical CO2 sorption on various coals.* International Journal of Coal Geology, **69**(4): p. 229-242, (2007).
15. Gensterblum, Y., et al., *European inter-laboratory comparison of high pressure CO2 sorption isotherms II: Natural coals.* International Journal of Coal Geology, **84**(2): p. 115-124, (2010).
16. Pini, R., S. Ottiger, L. Burlini, G. Storti, and M. Mazzotti, *Sorption of carbon dioxide, methane and nitrogen in dry coals at high pressure and moderate temperature.* International Journal of Greenhouse Gas Control, **4**(1): p. 90-101, (2010).
17. Han, F., A. Busch, B.M. Krooss, Z. Liu, and J. Yang, *CH4 and CO2 sorption isotherms and kinetics for different size fractions of two coals.* Fuel, **108**: p. 137-142, (2013).
18. Merkel, A., Y. Gensterblum, B.M. Krooss, and A. Amann, *Competitive sorption of CH4, CO2 and H2O on natural coals of different rank.* International Journal of Coal Geology, **150**: p. 181-192, (2015).
19. Pone, J.D.N., P.M. Halleck, and J.P. Mathews, *Sorption capacity and sorption kinetic measurements of CO2 and CH4 in confined and unconfined bituminous coal.* Energy & Fuels, **23**(9): p. 4688-4695, (2009).
20. Busch, A., Y. Gensterblum, B.M. Krooss, and R. Littke, *Methane and carbon dioxide adsorption–diffusion experiments on coal: upscaling and modeling.* International Journal of Coal Geology, **60**(2-4): p. 151-168, (2004).
21. Gruszkiewicz, M., M. Naney, J. Blencoe, D.R. Cole, J.C. Pashin, and R.E. Carroll, *Adsorption kinetics of CO2, CH4, and their equimolar mixture on coal from the Black Warrior Basin, West-Central Alabama.* International Journal of Coal Geology, **77**(1-2): p. 23-33, (2009).
22. Busch, A., Y. Gensterblum, B.M. Krooss, and N. Siemons, *Investigation of high-pressure selective adsorption/desorption behaviour of CO2 and CH4 on coals: An experimental study.* International Journal of Coal Geology, **66**(1-2): p. 53-68, (2006).
23. Marecka, A. and A. Mianowski, *Kinetics of CO2 and CH4 sorption on high rank coal at ambient temperatures.* Fuel, **77**(14): p. 1691-1696, (1998).
24. Siemons, N., K.-H.A. Wolf, and J. Bruining, *Interpretation of carbon dioxide diffusion behavior in coals.* International Journal of Coal Geology, **72**(3-4): p. 315-324, (2007).
25. Staib, G., R. Sakurovs, and E.M.A. Gray, *Dispersive diffusion of gases in coals. Part II: An assessment of previously proposed physical mechanisms of diffusion in coal.* Fuel, **143**: p. 620-629, (2015).
26. Zagorščak, R., *An investigation of coupled processes in coal in response to high pressure gas injection*, Ph. D. thesis, Cardiff University, Wales, UK, (2017).
27. Zagorščak, R. and H.R. Thomas, *Effects of subcritical and supercritical CO2 sorption on deformation and failure of high-rank coals.* International Journal of Coal Geology, **199**: p. 113-123, (2018).
28. ASTM Standards, *ASTM D2013. Standard Practice for preparing coal samples for analysis.* ASTM International, **05.06**(West Conshohocken, PA), (2013).
29. ASTM Standards, *ASTM D388. Standard Classification of Coals by Rank.* ASTM International, **05.06**(West Conshohocken, PA), (2015).
30. Sudibandriyo, M., Z. Pan, J.E. Fitzgerald, R.L. Robinson, and K.A. Gasem, *Adsorption of methane, nitrogen, carbon dioxide, and their binary mixtures on dry activated carbon at 318.2 K and pressures up to 13.6 MPa.* Langmuir, **19**(13): p. 5323-5331, (2003).

31. Mohammad, S., J. Fitzgerald, R.L. Robinson Jr, and K.A. Gasem, *Experimental uncertainties in volumetric methods for measuring equilibrium adsorption.* Energy & Fuels, **23**(5): p. 2810-2820, (2009).
32. Busch, A. and Y. Gensterblum, *CBM and CO2-ECBM related sorption processes in coal: a review.* International Journal of Coal Geology, **87**(2): p. 49-71, (2011).
33. Gathitu, B.B., W.-Y. Chen, and M. McClure, *Effects of coal interaction with supercritical CO2: physical structure.* Industrial & Engineering Chemistry Research, **48**(10): p. 5024-5034, (2009).
34. Lutynski, M.A., E. Battistutta, H. Bruining, and K.-H.A. Wolf, *Discrepancies in the assessment of CO 2 storage capacity and methane recovery from coal with selected equations of state Part I. Experimental isotherm calculation.* Physicochemical Problems of Mineral Processing, **47**, (2011).
35. Span, R. and W. Wagner, *A new equation of state for carbon dioxide covering the fluid region from the triple-point temperature to 1100 K at pressures up to 800 MPa.* Journal of physical and chemical reference data, **25**(6): p. 1509-1596, (1996).
36. Fitzgerald, J., Z. Pan, M. Sudibandriyo, R. Robinson Jr, K. Gasem, and S. Reeves, *Adsorption of methane, nitrogen, carbon dioxide and their mixtures on wet Tiffany coal.* Fuel, **84**(18): p. 2351-2363, (2005).
37. Langmuir, I., *The adsorption of gases on plane surfaces of glass, mica and platinum.* Journal of the American Chemical society, **40**(9): p. 1361-1403, (1918).
38. Clarkson, C. and R. Bustin, *The effect of pore structure and gas pressure upon the transport properties of coal: a laboratory and modeling study. 2. Adsorption rate modeling.* Fuel, **78**(11): p. 1345-1362, (1999).
39. Katyal, S., M. Valix, and K. Thambimuthu, *Study of parameters affecting enhanced coal bed methane recovery.* Energy Sources, Part A, **29**(3): p. 193-205, (2007).
40. Vandamme, M., L. Brochard, B. Lecampion, and O. Coussy, *Adsorption and strain: the CO2-induced swelling of coal.* Journal of the Mechanics and Physics of Solids, **58**(10): p. 1489-1505, (2010).
41. Ozdemir, E., B.I. Morsi, and K. Schroeder, *Importance of volume effects to adsorption isotherms of carbon dioxide on coals.* Langmuir, **19**(23): p. 9764-9773, (2003).
42. Battistutta, E., P. Van Hemert, M. Lutynski, H. Bruining, and K.-H. Wolf, *Swelling and sorption experiments on methane, nitrogen and carbon dioxide on dry Selar Cornish coal.* International Journal of Coal Geology, **84**(1): p. 39-48, (2010).
43. Fowler, P. and R. Gayer, *The association between tectonic deformation, inorganic composition and coal rank in the bituminous coals from the South Wales coalfield, United Kingdom.* International Journal of Coal Geology, **42**(1): p. 1-31, (1999).
44. Frodsham, K. and R. Gayer, *The impact of tectonic deformation upon coal seams in the South Wales coalfield, UK.* International journal of coal geology, **38**(3-4): p. 297-332, (1999).
45. Frodsham, K. and R. Gayer, *Variscan compressional structures within the main productive coal-bearing strata of South Wales.* Journal of the Geological Society, **154**(2): p. 195-208, (1997).

Supporting information for publication: